Radiation Measurements 90 (2016) 117–121

Contents lists available at ScienceDirect

Radiation Measurements

journal homepage: www.elsevier.com/locate/radmeas

Positron trapping defects in free-volume investigation of Ge–Ga–S–CsCl glasses

H. Klym [a, *], A. Ingram [b], O. Shpotyuk [c, d], O. Hotra [e], A.I. Popov [f]

[a] Lviv Polytechnic National University, 12, Bandera str., Lviv, 79013, Ukraine
[b] Opole University of Technology, 75, Ozimska str., Opole, 45370, Poland
[c] Vlokh Institute of Physical Optics, 23, Dragomanov str., 79005, Lviv, Ukraine
[d] Jan Dlugosz University, 13/15, al. Armii Krajowej, Czestochowa, 42201, Poland
[e] Lublin University of Technology, 38A ul. Nadbystrzycka, 20-618, Lublin, Poland
[f] Institute of Solid State Physics, University of Latvia, 8, Kengaraga, Riga, LV-1063, Latvia

HIGHLIGHTS

- CsCl additives in Ge–Ga–S glassy matrix lead to the agglomeration of voids.
- Full crystallization of Ge–Ga–S–CsCl glasses corresponds to the formation of defect voids.
- Gamma-irradiation of glass stimulates the creation of additional defects and darkening.

ARTICLE INFO

Article history:
Received 25 October 2015
Received in revised form
12 January 2016
Accepted 19 January 2016
Available online 21 January 2016

Keywords:
Chalcogenide glass
Alkali halide
Positron trapping
Free-volume defects
Crystallization

ABSTRACT

Evolution of free-volume positron trapping defects caused by crystallization process in $(80GeS_2-20Ga_2S_3)_{100-x}(CsCl)_x$, $0 \le x \le 15$ chalcogenide-chalcohalide glasses was studied by positron annihilation lifetime technique. It is established that CsCl additives in Ge–Ga–S glassy matrix transform defect-related component spectra, indicating that the agglomeration of free-volume voids occurs in initial and crystallized $(80GeS_2-20Ga_2S_3)_{100-x}(CsCl)_x$, $0 \le x \le 10$ glasses. Void fragmentation in $(80GeS_2-20Ga_2S_3)_{85}(CsCl)_{15}$ glass can be associated with loosing of their inner structure. Full crystallization in each of these glasses corresponds to the formation of defect-related voids. These trends are confirmed by positron-positronium decomposition algorithm. It is shown, that CsCl additives result in white shift in the visible regions in transmission spectra. The γ-irradiation of $80GeS_2-20Ga_2S_3$ base glass leads to slight long-wavelength shift of the fundamental optical absorption edge and decreasing of transmission speaks in favor of possible formation of additional defects in glasses and their darkening.

1. Introduction

Chalcogenide glass (ChG) materials with improved exploitation properties are important for novel applications (Ailavajhala et al., 2014; Petit et al., 2008; Richardson et al., 2010). Unique multi-functionality of $GeS_2-Ga_2S_3$ ChG family manifests in luminescence phenomena, *e.g.* intense radioactive photoemission of rear-earth doping additives introduced in modified ChG (Kostka et al., 2015; Zhang et al., 2014; Seddon et al., 2010), ion-conductive phenomena, *e.g.* abnormal conductivity of Li^+ ions in solid electrolytes (Ren et al., 2011) and diffusive-related phenomena, *e.g.* reversible self-healing effects observed in photoinduced refraction owing to ion-conducting additives (Yao and Martin, 2008).

In all the above cases, only optimized defect inner-pore structure of basic $GeS_2-Ga_2S_3$ ChG defines their final glassy-like state – its extended functionality connected with the possibility to accommodate outer atoms and their groups. It is of high importance that by controlled halide (CsCl) addition these ChG can be easily transformed in chalcogenide ceramics transparent in IR region, as it was well demonstrated in (Yao and Martin, 2008). In addition, the compositional series of ChG can range from model binary (GeS_2, As_2S_3) to ecologically-friendly Ga-doped quasi-binary $GeS_2-Ga_2S_3$ systems as host matrix for rear-earth activators, and then modified with alkali halides MX (M = Cs, X = Cl) (Calvez et al.,

* Corresponding author.
E-mail address: klymha@yahoo.com (H. Klym).

http://dx.doi.org/10.1016/j.radmeas.2016.01.023
1350-4487/

2007) to ensure functionality in visible range and activated by rear-earth ions (Dy^{3+} or Pr^{3+}) to produce highly-efficient photonics media (Lu et al., 2014).

However, the functionality mechanism of these systems is yet unknown because their free-volume defect-related structure has not been investigated, significantly limiting the further progress in modern IR photonics. It is well-known, that the nearest atomic arrangement in a glasses, ceramics and nanomaterials can be adequately studied with numerous experimental measuring methods (like vibration and Raman scattering spectroscopy, XRD, SEM, XPS, XAFS, XANES, NMR, etc.) (Purans et al., 1987; Majid et al., 1998; Karbovnyk et al., 2014; Bellucci et al., 2008; Balasubramanian et al., 2006; Bellucci et al., 2007; Popov et al., 2013). However, the choice of probes available to study atomic-deficient distribution is rather limited, especially at sub-nanometer scale. One of the best techniques capable to probe such finest free volumes is the positron annihilation lifetime (PAL) spectroscopy, a well-approved tool to study atomic void structure (nucleates, fragmentation, vacancy clusters, etc.) in binary ChG (Golovchak et al., 2013). In this work, we are analyzing free-volume defects and voids in as-prepared and crystallized nanostructurally modified mixed chalcohalide glassy compounds of ChG-MX type $((80GeS_2{-}20Ga_2S_3)_{100-x}(CsCl)_x$, $0 \le x \le 15$) using PAL technique. The x3-x2-decomposition algorithm proposed in (Shpotyuk et al., 2015) is used in this work to analyze free-volume nanostructured media caused by crystallization processes in the host $GeS_2{-}Ga_2S_3{-}CsCl$ matrix.

2. Experimental

$GeS_2{-}Ga_2S_3{-}CsCl$ glasses were prepared from Ge, Ga, S and CsCl materials in silica ampoule kept under 10^{-6} Pa vacuum, as described earlier in (Calvez et al., 2010; Shpotyuk et al., 2014). Materials were melted at 850 °C in a silica tube for several hours. The $(80GeS_2{-}20Ga_2S_3)_{100-x}(CsCl)_x$, $0 \le x \le 15$ glasses were annealed at 15 °C below glass transition temperature T_g for all glasses (Masselin et al., 2012) to minimize inner strains. The crystallization of ChG was carried out at thermal annealing at (T_g + 30 °C). It was found that after such processing the complete crystallization of samples occurred.

The influence of γ-irradiation on optical properties of base $80GeS_2{-}20Ga_2S_3$ ChG was investigated using Co^{60} source. The dose of γ-irradiation was near 0.8 MGy, and the total duration of this procedure was 2 months.

Transformation of free-volume defects and voids in $(80GeS_2{-}20Ga_2S_3)_{100-x}(CsCl)_x$, $0 \le x \le 15$ glasses was investigated by PAL method using ORTEC spectrometer (positron source – ^{60}Co isotope) at 22 °C and relative humidity of 35%. Each spectrum was measured for two identical samples with a channel width of 6.15 ps and analyzed using LT 9.0 computer program (Kansy, 1996).

In our previous work (Shpotyuk et al., 2015), we used a two-component fitting procedure to reconstruct the measured PAL spectra, this being achieved by corresponding choice of source contribution. The improved statistical treatment in this research for a majority of the studied samples testifies that three-component unconstrained fitting has an obvious preference in view of better approximation for PAL spectra. Thus, the best results were obtained using model of three components with lifetimes τ_1, τ_2, τ_3 and intensities I_1, I_2, I_3 reflecting positron and positronium (ortho-positronium trapping) parameters (Krause-Rehberg and Leipner, 1999; Jean et al., 2003). The first component with τ_1 and I_1 is of no physical meaning, positron trapping in free-volume entities and defects corresponds to the second component (τ_2, I_2). The third component (τ_3, I_3) in the envelope of the fitting curves corresponds to positronium formation. PAL experiment and peculiarities of mathematical treatment is described in details elsewhere (Golovchak et al., 2013; Shpotyuk et al., 2014; Klym et al., 2014; Filipecki et al., 2007).

Positron trapping parameters such as average positron lifetime τ_{av}, defect-free positron lifetime τ_b and positron trapping rate in defects κ_d were calculated using well-known positron-trapping model (Krause-Rehberg and Leipner, 1999; Alatalo et al., 1996). The $(\tau_2 - \tau_b)$ difference demonstrates size of free-volume defects where positrons are trapped, and the τ_2/τ_b ratio reflects the nature of these defects.

Nanostructurization of $GeS_2{-}Ga_2S_3{-}CsCl$ glasses due to full crystallization was characterized using the x3-x2-decomposition algorithm as an indicator of positron-positronium transformation in host and modified matrix. Methodological approach to the implementation of this algorithm was discussed in (Shpotyuk et al., 2015).

3. Results and discussion

As depicted in Fig. 1, the addition of CsCl results in white shift in the visible regions, in agreement with (Masselin et al., 2012). The transmission increases with CsCl concentration from 75% in $(CsCl)_0$–80% in $(CsCl)_{10}$ and $(CsCl)_{15}$. By adding up to 15% mol. of the alkali halide in the glassy matrix, the band-gap evolves from 2.64 eV to 2.91 eV. From a structural point of view, the addition of less than 15% of CsCl in $GeS_2{-}Ga_2S_3$ glasses is characterized by the formation of $GaS_{4-x}Cl_x$ tetrahedra that are dispersed in the glass network (Masselin et al., 2012). The average number of Ga–S bands decreases in favor of the average number of Ga–Cl bonds.

The slight long-wavelength shift of the fundamental optical absorption edge and the decrease in transmission are observed in glasses after γ-irradiation with dose near 0.8 MGy during 2 months (Fig. 2). This indicates possible formation of additional defects in $80GeS_2{-}20Ga_2S_3$ ChG and their darkening. In other worlds, after γ-irradiation, nanovoids with different size are created as intrinsic structural defects associated with topologically uncoordinated negative-changed centers. These defect centers form additional energy levels both near the bottom of the conduction band and in the vicinity of the valence band, as well as additional intrinsic electric fields. The mechanism of irradiation-induced darkening of $80GeS_2{-}20Ga_2S_3$ ChG is connected with oxidation processes most probably related with the appearance of GeS_2 phase at the surface of the glasses.

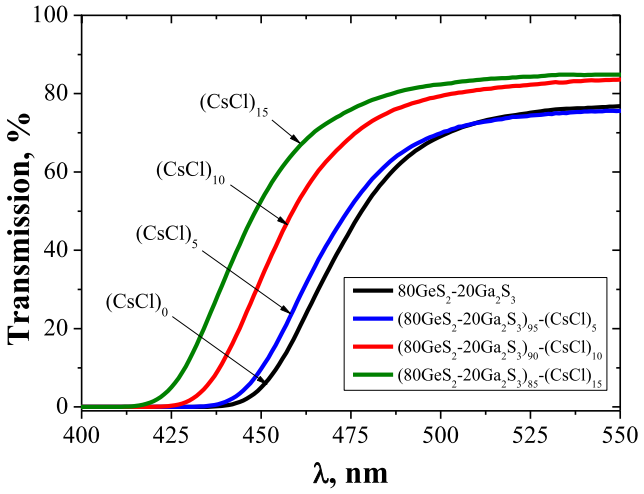

Fig. 1. Transmission spectra in the visible region of $(80GeS_2{-}20Ga_2S_3)_{100-x}(CsCl)_x$, $0 \le x \le 15$ glasses.

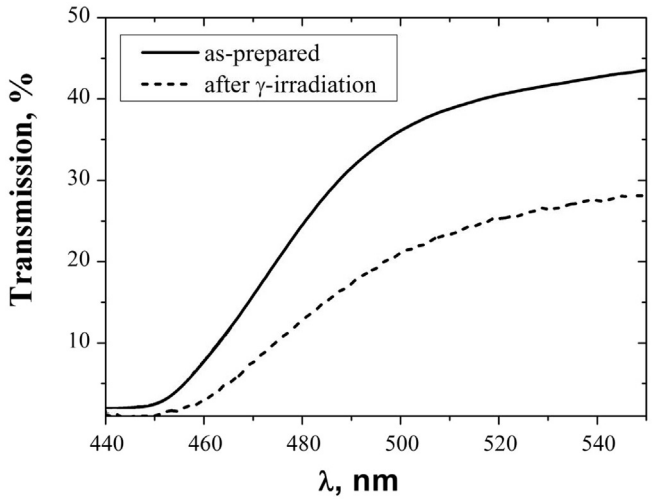

Fig. 2. Transmission spectra for as-prepared and γ-irradiated $80GeS_2–20Ga_2S_3$ base glasses.

PAL spectrum for quasi-binary $GeS_2–Ga_2S_3$ glassy matrix deconvoluted into three components is shown in Fig. 3. Mathematically, this curve can be represented as a sum of three exponential decay functions with the powers inversely proportional to positron lifetimes τ_1, τ_2 and τ_3 and the area under each of these exponential curves being proportional to the intensities I_1, I_2 and I_3 (Bigg, 1996).

The fitting parameters and positron trapping modes for PAL spectra of as-prepared and crystallized $(80GeS_2–20Ga_2S_3)_{100-x}(CsCl)_x$, $0 \le x \le 15$ glasses are given in Table 1 and Table 2, correspondingly. As shown earlier in (Shpotyuk et al., 2014; Klym et al., 2015), the first component with the parameters τ_1 and I_1 has no physical meaning for ChG. The third component reflects ortho-positronium decaying in solids (Klym et al., 2014; Filipecki et al., 2007). The I_3 intensity is at the level of statistical deviation (~1÷3%), but this component is needed for the calculation of PAL data within x3-x2-decomposition algorithm. Therefore, the main attention will be focused on the second defect-related component (τ_2, I_2). The lifetime τ_2 represents the size of the free-volume defects and voids in the inner structure of glasses and

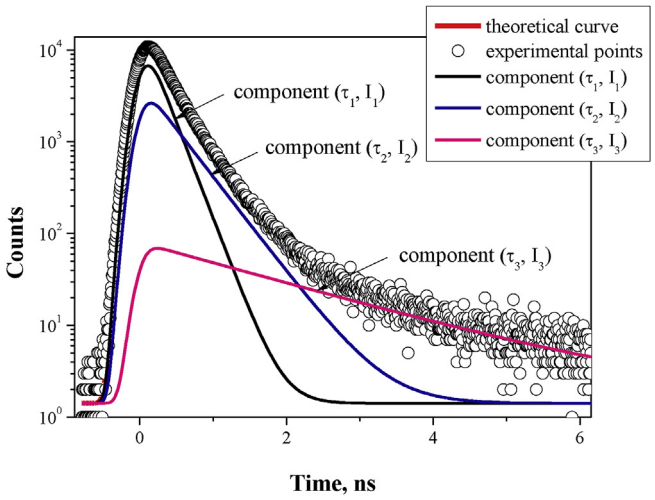

Fig. 3. Typical PAL spectrum for Ge–Ga–S–CsCl glasses decomposed into three combined positron-positronium components.

Table 1
Comparison of fitting parameters for PAL spectra for as-prepared and crystallized $(80GeS_2–20Ga_2S_3)_{100-x}(CsCl)_x$, $0 \le x \le 15$ glasses.

Sample pre-history	τ_1, ns	I_1, a.u.	τ_2, ns	I_2, a.u.	τ_3, ns	I_3, a.u.
$80GeS_2–20Ga_2S_3$						
as-prepared	0.201	0.581	0.426	0.387	1.958	0.032
crystallized	0.217	0.598	0.401	0.380	1.904	0.022
$(80GeS_2–20Ga_2S_3)_{95}(CsCl)_5$						
as-prepared	0.234	0.639	0.462	0.339	1.978	0.022
crystallized	0.221	0.699	0.424	0.287	2.026	0.014
$(80GeS_2–20Ga_2S_3)_{90}(CsCl)_{10}$						
as-prepared	0.249	0.696	0.499	0.290	2.029	0.014
crystallized	0.232	0.695	0.446	0.292	1.948	0.013
$(80GeS_2–20Ga_2S_3)_{85}(CsCl)_{15}$						
as-prepared	0.240	0.712	0.496	0.270	2.206	0.018
crystallized	0.221	0.605	0.431	0.380	1.952	0.015

Table 2
Positron trapping parameters for PAL spectra of as-prepared and crystallized $(80GeS_2–20Ga_2S_3)_{100-x}(CsCl)_x$, $0 \le x \le 15$ glasses.

Sample pre-history	τ_{av}., ns	τ_b, ns	κ_d, ns	$\tau_2 - \tau_b$, ns^{-1}	τ_2/τ_b
$80GeS_2–20Ga_2S_3$					
as-prepared	0.291	0.255	1.05	0.17	1.67
crystallized	0.282	0.255	0.91	0.15	1.57
$(80GeS_2–20Ga_2S_3)_{95}(CsCl)_5$					
as-prepared	0.313	0.282	0.73	0.18	1.64
crystallized	0.280	0.257	0.63	0.17	1.65
$(80GeS_2–20Ga_2S_3)_{90}(CsCl)_{10}$					
as-prepared	0.322	0.292	0.59	0.21	1.71
crystallized	0.295	0.270	0.61	0.18	1.65
$(80GeS_2–20Ga_2S_3)_{85}(CsCl)_{15}$					
as-prepared	0.310	0.279	0.59	0.22	1.77
crystallized	0.302	0.272	0.85	0.16	1.59

the intensity I_2 is proportional to the number of these defects.

It is shown that for as-prepared glasses the increase of CsCl additive in host $80GeS_2–20Ga_2S_3$ matrix results in the rise of lifetime τ_2 and drop of intensity I_2. The value of the main positron trapping parameter – positron trapping rate in defects κ_d decreases mainly due to the changes in I_2 (Fig. 4,a,b). Such changes in intrinsic defect-related structure of Ge–Ga–S glasses caused by CsCl alkali halides can be constrained by processes of atomic-deficit void agglomeration. Thus, CsCl additive results in the expansion of free volumes in ChG, which is a favorable condition for future modification of glassy matrix by rare-earth elements.

As compared to as-prepared and crystallized (or ceramized) ChG for each of the glass compositions, different tendencies in transformation of defect-related fitting parameters and positron trapping modes are observed. After crystallization of $80GeS_2–20Ga_2S_3$ base glass, the lifetime τ_2 shows decrease from 0.426 ns to 0.401 ns and intensity I_2 also insignificant reduces (Fig. 4,a). This means that at full crystallization of base Ge–Ga–S glasses, the free-volume defects contracts and, simultaneously, their total number decrease. In other words, free-volume defect-related voids got in an unfavorable environment and the efficiency of positron trapping degrades through the exclusion or reduction of some part of free volume. Schematic illustration of void contraction and agglomeration is shown in Fig. 5. In the case of $(80GeS_2–20Ga_2S_3)_{95}(CsCl)_5$ glasses the revealed changes are more evident. But in $(80GeS_2–20Ga_2S_3)_{90}(CsCl)_{10}$ ChG the increasing of defect-related lifetime τ_2 is accompanied by pretty stable values of intensities I_2 in as-prepared and crystallized glasses (Table 1). So, the size of voids decreases but their amount is fixed. Observed transformation can be explained by void shrinking or contraction through the formation of favorable environment for transformation of voids in size without significant changes in positron trapping effectiveness.

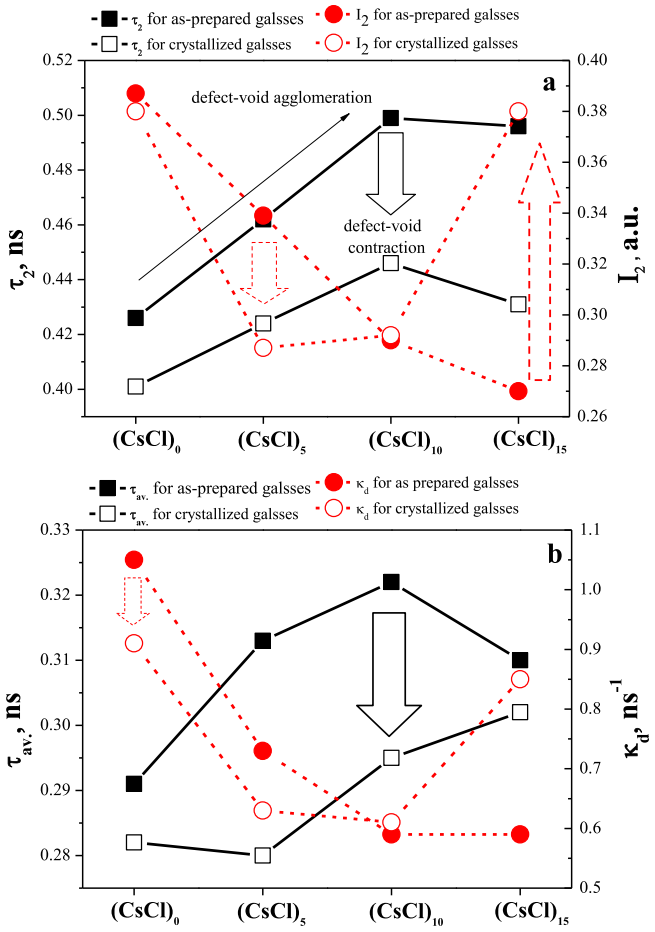

Fig. 4. Defect-related (τ_2, I_2) component (a) and average lifetime $\tau_{av.}$ and positron trapping rate κ_d in defects (b) for as-prepared and crystallized GeS_2–Ga_2S_3–CsCl glasses as function of CsCl content.

(Shpotyuk et al., 2014). Probably, chalcohalide $GeSe_2$–Ga_2Se_3–CsCl glasses with larger amount of CsCl exhibited some inner free-volume transformation already during their preparation. At such conditions the crystallization was not completed. Thus, the evolution of free-volume voids occurred due to the same mechanism as in Ge–Ga–Se glasses under long-term thermally-induced influences.

Through the comparison of defect-related parameters for crystallized $(80GeS_2–20Ga_2S_3)_{100-x}(CsCl)_x$, $0 \le x \le 10$ glasses, it is established that lifetime τ_2 rises and intensity I_2 reduces with CsCl addition. As it was in the case of as-prepared glasses of the same compositions this confirms the agglomeration process of voids in their inner structure. The ratio τ_2/τ_b that falls within 1.6–1.7 demonstrates positron trapping in centers most probably as di/tri-atomic vacancies (Ingram et al., 2012).

In addition, crystallization processes of CsCl-containing Ge–Ga–S chalcogenide glasses were studied within proposed x3-x2-decomposition algorithm (Shpotyuk et al., 2015). As-prepared $(80GeS_2–20Ga_2S_3)_{100-x}(CsCl)_x$, $0 \le x \le 15$ glasses were taken as host matrices and crystallized ChG of every composition were defined as nanostructurally modified matrices. Within such approach (τ_n, I_n) and (τ_{int}, I_{int}) components were described as physical parameterization of nanoparticle-connected sites in crystallized glasses within two-term decomposed PAL spectrum (Shpotyuk et al., 2015). The defect-related lifetime τ_{int} reflects positron trapping sites due to embedded CsCl and nanoparticle formed after crystallization. The calculated results are shown in Table 3. Increasing of τ_{int} and I_{int} parameters for $80GeS_2–20Ga_2S_3$ and $(80GeS_2–20Ga_2S_3)_{95}(CsCl)_5$ glasses after their full crystallization proves decoarsening or contraction of defect-related voids. Application of x3-x2-decomposition treatment to $(80GeS_2–20Ga_2S_3)_{90}(CsCl)_{10}$ ChG has lead to the negative values of lifetimes. This demonstrates the limitation of x3-x2 algorithm to describing of inner structural transformations caused by shortening of nanovoids. Crystallization of $(80GeS_2–20Ga_2S_3)_{85}(CsCl)_{15}$ glasses is accompanied by void fragmentation. Corresponding changes

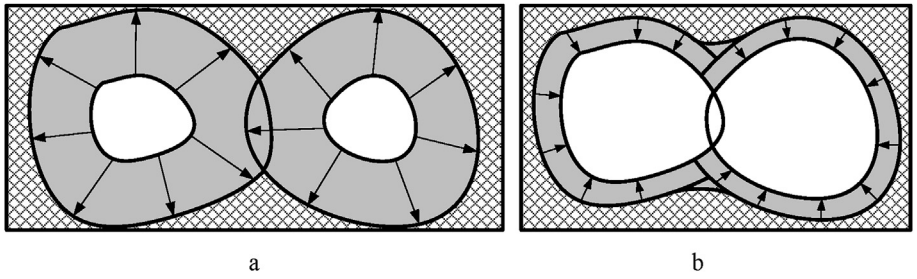

Fig. 5. Schematic illustration of free-volume void agglomeration due to modification of Ge–Ga–S glassy matrix by CsCl addition (a) and void constriction (b) caused by full crystallization process.

The values of positron trapping modes such as $\tau_{av.}$, τ_b, κ_d and difference ($\tau_2 - \tau_b$) reflecting size of defects decrease in crystallized base glasses and with CsCl additives (Table 2).

Largest amount of CsCl (x = 15) in Ge–Ga–S matrix result in loosening of their structure. Therefore, another tendency has been observed for $(80GeS_2–20Ga_2S_3)_{85}(CsCl)_{15}$ ChG after crystallization. So, lifetime τ_2 decreases from 0.496 ns to 0.431 ns in as-prepared and crystalized ChG, respectively, while intensity I_2 and positron trapping rate in defects κ_d increase after full crystallization of glasses. Such transformation demonstrates agglomeration of defect-related inner voids into large amount of smaller defects like at crystallization in pseudo-binary $GeSe_2$–Ga_2Se_3 systems reflect higher value of the lifetime τ_{int} in comparison with the host as-prepared matrix, while positron-trapping rate in defects κ_d is closer to crystallized glasses of same compositions.

4. Conclusion

In this paper, the experimental study of defect-related void changes in $(80GeS_2–20Ga_2S_3)_{100-x}(CsCl)_x$, $0 \le x \le 15$ glasses has been performed by PAL method. The obtained spectra were deconvoluted into two positron-trapping (τ_1, I_1) and (τ_2, I_2) components and one positronium decaying (τ_3 I_3) component. It is found that lifetime τ_2, intensity I_2 and positron trapping rate in

Table 3
PAL parameters of "pure" trapping for $(80GeS_2–20Ga_2S_3)_{100-x}(CsCl)_x$, $0 \le x \le 15$ glasses caused by their crystallization calculated within x3-x2-decomposition algorithm (host matrix is as-prepared glasses each compositions, modified matrix – crystallized glasses of each compositions).

Sample	τ_n, ns	I_n, a.u.	τ_{int}, ns	I_{int}, a.u.	$\tau_{av.}$, ns	τ_b, ns	κ_d, ns^{-1}	$\tau_2 - \tau_b$, ns	τ_2/τ_b
$(CsCl)_0$	0.282	0.117	0.343	0.114	0.312	0.309	0.311	0.034	1.110
$(CsCl)_5$	0.176	0.159	0.309	0.071	0.217	0.203	0.762	0.106	1.524
$(CsCl)_{10}$	−0.189	0.027	−0.182	0.023	−0.186	−0.186	0.092	0.004	0.980
$(CsCl)_{15}$	0.190	0.224	0.337	0.155	0.250	0.231	0.944	0.106	1.458

defects κ_d decrease after crystallization for each of the glasses. This result indicates the transformation of void agglomerates with alkali halide CsCl additive into specific void contractions. Other trends are observed in $(80GeS_2–20Ga_2S_3)_{85}(CsCl)_{15}$ glasses with loosed structure, where void fragmentation occurs after their crystallization. The x3-x2 decomposition algorithm gives information about "pure" trapping in modified matrix and confirms obtained PAL results.

Acknowledgments

H. Klym thank the Lviv Polytechnic University under Doctoral Program and support via Project DB/KIBER (No 0115U000446), while A.I. Popov thanks VBBKC L-KC-11-0005 project Nr.KC/2.1.2.1.1/10/01/006, 5.4 for a funding.

References

Ailavajhala, M.S., Gonzalez-Velo, Y., Poweleit, C.D., Barnaby, H.J., Kozicki, M.N., Butt, D.P., Mitkova, M., 2014. New functionality of chalcogenide glasses for radiation sensing of nuclear wastes. J. Hazard. Mater. 269, 68–73.

Alatalo, M., Barbiellini, B., Hakala, M., Kauppinen, H., Korhonen, T., Puska, M.J., Saarinen, K., Hautojarvi, P., Nieminen, R.M., 1996. Theoretical and experimental study of positron annihilation with core electrons in solids. Phys. Rev. B 54 (4), 2397–2409.

Balasubramanian, C., Bellucci, S., Cinque, G., Marcelli, A., Cestelli Guidi, M., Piccinini, M., Popov, A., Soldatov, A., Onorato, P., 2006. Characterization of aluminium nitride nanostructures by XANES and FTIR spectroscopies with synchrotron radiation. J. Phys. Condens. Matter 18 (33), S2095.

Bellucci, S., Popov, A.I., Balasubramanian, C., Cinque, G., Marcelli, A., Karbovnyk, I., Savchyn, V., Krutyak, N., 2007. Luminescence, vibrational and XANES studies of AlN nanomaterials. Radiat. Meas. 42 (4), 708–711.

Bellucci, S., Bolesta, I., Karbovnyk, I., Hrytskiv, R., Fafilek, G., Popov, A.I., 2008. Microstructure of Ag_2BI_4(B=Ag,Cd) superionics studied by SEM, impedance spectroscopy and fractal dimension analysis. J. Phys. Condens. Matter 20 (47), 474211.

Bigg, M., 1996. A review of positron annihilation lifetime spectroscopy as applied to the physical ageing of polymers. Eng. Sci. 36 (6), 737–743.

Calvez, L., Lucas, P., Rozé, M., Ma, H.L., Lucas, J., Zhang, X.H., 2007. Influence of gallium and alkali halide addition on the optical and thermo-mechanical properties of $GeSe_2$-Ga_2Se_3 glass. Appl. Phys. A 89, 183–188.

Calvez, L., Lin, C., Rozé, M., Ledemi, Y., Guillevic, E., Bureau, B., Allix, M., Zhang, X., 2010. Similar behaviors of sulfide and selenide-based chalcogenide glasses to form glass-ceramics. Proc. SPIE 7598, 759802-1-16.

Filipecki, J., Ingram, A., Klym, H., Shpotyuk, O., Vakiv, M., 2007. Water-sensitive positron trapping modes in nanoporous magnesium aluminate ceramics. J. Phys. Conf. Ser. 79 (1), 012015.

Golovchak, R., Ingram, A., Kozyukhin, S., Shpotyuk, O., 2013. Free volume fragmentation in glassy chalcogenides during natural physical ageing as probed by PAL spectroscopy. J. Non-cryst. Solids 377, 49–53.

Ingram, A., Golovchak, R., Kostrzewa, M., Wacke, S., Shpotyuk, M., Shpotyuk, O., 2012. Compositional dependences of average positron lifetime in binary As–S/Se glasses. Phys. B 407, 652–655.

Jean, Y.C., Mallon, P.E., Schrader, D.M., 2003. Principles and Application of Positron and Positronium Chemistry. World Scientific, Singapore.

Kansy, J., 1996. Microcomputer program for analysis of positron annihilation lifetime spectra. Nucl. Instr. Methods Phys. Res. A 374, 235–244.

Karbovnyk, I., Bolesta, I., Rovetskii, I., Velgosh, S., Klym, H., 2014. Studies of CdI_2-Bi_3 microstructures with optical methods, atomic force microscopy and positron annihilation spectroscopy. Mater. Sci. Pol. 32 (3), 391–395.

Klym, H., Ingram, A., Hadzaman, I., Shpotyuk, O., 2014. Evolution of porous structure and free-volume entities in magnesium aluminate spinel ceramics. Ceram. Int. 40, 8561–8576.

Klym, H., Ingram, A., Shpotyuk, O., Calvez, L., Petracovschi, E., Kulyk, B., Serkiz, R., Szatanik, R., 2015. "Cold" crystallization in nanostructurized $80GeSe_2$-$20Ga_2Se_3$ glass. Nanoscale Res. Lett. 10, 49.

Kostka, P., Zavadil, J., Iovu, M.S., Ivanova, Z.G., Furniss, D., Seddon, A.B., 2015. Low-temperature photoluminescence in chalcogenide glasses doped with rare-earth ions. J. Alloys Compd. 648, 237–243.

Krause-Rehberg, R., Leipner, H., 1999. Positron Annihilation in Semiconductors. Springer, Heidelberg.

Lu, C., Guo, H., Xu, Y., Hou, C., Lu, M., He, X., Peng, B., 2014. Mid-infrared emissions of Pr^{3+}-doped GeS_2–Ga_2S_3–CdI_2 chalcohalide glasses. Mater. Res. Bull. 60, 391–396.

Majid, M., Benazeth, S., Souleau, C., Purans, J., 1998. XAFS study of interchain and intrachain order in $Se_{1-x}Te_x$ glasses: nearest neighbors. Phys. Rev. B 58 (10), 6104.

Masselin, P., Le Coq, D., Calvez, L., Petracovschi, E., Lepine, E., Bychkov, E., Zhang, X., 2012. CsCl effect on the optical properties of the $80GeS_2$–$20Ga_2S_3$ base glass. Appl. Phys. A 106, 697–702.

Petit, L., Carlie, N., Anderson, T., Choi, J., Richardson, M., Richardson, K.C., 2008. Progress on the photoresponse of chalcogenide glasses and films to near-infrared femtosecond laser irradiation: a Review. IEEE J. Sel. Top. Quantum Electron. 14 (5), 1323–1334.

Popov, A.I., Shirmane, L., Pankratov, V., Lushchik, A., Kotlov, A., Serga, V.E., Kulikova, L.D., Chikvaidze, G., Zimmermann, J., 2013. Comparative study of the luminescence properties of macro-and nanocrystalline MgO using synchrotron radiation. Nucl. Instrum. Methods B 310, 23–26.

Purans, J., Balzarotti, A., Motta, N., Menushenkov, A., 1987. EXAFS and XANES studies of local order in oxide glasses: manganese impurity defects and vanadium low symmetry complexes. J. Non-cryst. solids 94 (3), 336–344.

Ren, J., Wagner, T., Bartos, M., Frumar, M., Oswald, J., Kincl, M., Frumarova, B., Chen, G., 2011. Intense near-infrared and midinfrared luminescence from the Dy^{3+}-doped $GeSe_2$-Ga_2Se_3-MI (M=K, Cs, Ag) chalcohalide glasses at 1.32, 1.73, and 2.67 μm. J. Appl. Phys. 109, 033105.

Richardson, K., Krol, D., Hirao, K., 2010. Glasses for photonic applications. Inter. J. Appl. Glass Sci. 1 (1), 74–86.

Seddon, A.B., Tang, Z., Furniss, D., Sujecki, S., Benson, T.M., 2010. Progress in rare-earth-doped mid-infrared fiber lasers. Opt. Express 18, 26704–26719.

Shpotyuk, O., Calvez, L., Petracovschi, E., Klym, H., Ingram, A., Demchenko, P., 2014. Thermally-induced crystallization behaviour of $80GeSe_2$–$20Ga_2Se_3$ glass as probed by combined X-ray diffraction and PAL spectroscopy. J. Alloys Compd. 582, 323–327.

Shpotyuk, O., Filipecki, J., Ingram, A., Golovchak, R., Vakiv, M., Klym, H., Balitska, V., Shpotyuk, M., Kozdras, A., 2015. Positronics of subnanometer atomistic imperfections as high-informative characterization tool in nanomaterials science. Nanoscale Res. Lett. 10, 77.

Yao, W., Martin, S.W., 2008. Ionic conductivity of glasses in the MI+M_2S+($0.1Ga_2S_3$+$0.9GeS_2$) system (M=Li, Na, K and Cs. Solid State Ionics 178, 1777–1784.

Zhang, P., Dai, S., Niu, X., Xu, Y., Zhang, W., Wu, Y., Nie, Q., 2014. Design of rare-earth-ion doped chalcogenide photonic crystals for enhancing the fluorescence emission. Opt. Commun. 322, 123–128.